Int. J. Solids Structures, 1975, Vol. 11, pp. 647–663. Pergamon Press. Printed in Great Britain

BUCKLING OF ECCENTRICALLY STIFFENED ELASTIC-PLASTIC PANELS ON TWO SIMPLE SUPPORTS OR MULTIPLY SUPPORTED

VIGGO TVERGAARD
Department of Mathematics, Massachusetts Institute of Technology, Cambridge, MA 02139, U.S.A.

and

ALAN NEEDLEMAN
Department of Mathematics, Massachusetts Institute of Technology, Cambridge, MA. 02139, U.S.A.

(*Received* 8 *August* 1974; *in revised form* 30 *October* 1974)

Abstract—Buckling due to axial compression is investigated for elastic-plastic, stiffened wide panels either continuous in the longitudinal direction over several transverse supports or finite and supported along the two edges. An analytical treatment is given of the bifurcation behaviour and of the initial post-bifurcation behaviour of perfect panels compressed into the plastic range. The behaviour of initially imperfect panels is computed numerically using an incremental method. In each increment a linear problem is solved by a combined Rayleigh Ritz-finite element method. Computed examples show a considerable imperfection-sensitivity, both for panels that bifurcate in the plastic range, and for panels with a yield stress a little above the elastic bifurcation stress.

1. INTRODUCTION

The imperfection-sensitivity of an eccentrically stiffened elastic-plastic panel is partly due to interaction between the wide column buckling mode and a local buckling mode. In the elastic range the weakening effect of such mode interactions has been treated by van der Neut[1], Koiter and Kuiken[2] and Thompson and Lewis[3] for thin-walled columns and by Tvergaard[4, 5] and recently by other authors[6–8] for eccentrically stiffened wide panels. Graves–Smith[9] has considered mode interaction in an elastic-plastic thin-walled box-column, while in [10] the authors presented results for the post-bifurcation behaviour and imperfection-sensitivity of a wide eccentrically stiffened elastic-plastic panel simply supported on the two edges on which the compressive load acts. In [10] attention was focused on cases in which bifurcation of the perfect structure occurred in the plastic range.

Here, we consider both panels that are simply supported on the two edges on which the loading acts and, as is often the case in practice, panels that are continuous in the direction of applied compressive load and supported on several transverse supports. For these two sets of boundary conditions the bifurcation load is determined analytically and Hutchinson's asymptotic theory of post-bifurcation behaviour in the plastic range[11, 12] is employed to obtain approximate results for the maximum support load, for the corresponding buckling mode deflection and for the propagation of the elastic unloading regions after bifurcation. In all computations the stiffeners are treated as beams so that the stiffener cross-sections do not distort. The behaviour of panels with initial imperfections is computed numerically by a combined Rayleigh Ritz-finite element method and a comparison is made between the numerical efficiency of this method and a full Rayleigh Ritz calculation. Furthermore, the present paper contains some results for the effect of plastic yielding on imperfect panels designed so that bifurcation of the perfect structure occurs in the elastic range.

2. PROBLEM FORMULATION

The integrally stiffened panel is assumed to be infinitely wide in the x_2-direction with a constant spacing b between the stiffeners and is under axial compression in the x_1-direction (Fig. 1). The plate thickness is h, and the eccentricity e of the stiffeners is positive in the x_3-direction. The panel is either finite in the x_1-direction with the distance a between the simply supported edges as the panel considered in [10] or it is continuous over several transverse supports at distance a (Fig. 1).

The displacements of the plate middle surface in the x_1, x_2 and x_3 directions are denoted u_1, u_2 and w, respectively. Then, with the usual assumptions of von Kármán plate theory, the strain rates of the plate middle surface $\dot{\epsilon}_{\alpha\beta}$ and the bending strain rates $\dot{\kappa}_{\alpha\beta}$ are taken to be

$$\dot{\epsilon}_{\alpha\beta} = \frac{1}{2}(\dot{u}_{\alpha,\beta} + \dot{u}_{\beta,\alpha} + w_{,\alpha}\dot{w}_{,\beta} + \dot{w}_{,\alpha}w_{,\beta}), \quad \dot{\kappa}_{\alpha\beta} = \dot{w}_{,\alpha\beta} \tag{2.1}$$

where a dot denotes differentiation with respect to some monotonically increasing parameter that characterizes the load history. The centre line strain rate and the bending strain rate of a stiffener are taken to be

$$\dot{\epsilon}_s = \dot{u}_{1,1} - e\dot{w}_{,11} + w_{,1}\dot{w}_{,1} + e^2 w_{,12}\dot{w}_{,12}, \quad \dot{\kappa}_s = \dot{w}_{,11} \tag{2.2}$$

as in [4]. Here subscript s refers to a stiffener,but otherwise Latin indices range from 1 to 3, and Greek indices range from 1 to 2.

A small strain theory of plasticity is used in which the three dimensional stress rates and strain rates are assumed to be related by the equations

$$\dot{\sigma}_{ij} = L_{ijkl}\dot{\eta}_{kl} \tag{2.3}$$

with $L_{ijkl} = L_{jikl} = L_{klij}$. The instantaneous moduli L_{ijkl} depend on the stress history, and we assume that they have two branches depending on whether loading or unloading occurs. In the approximately plane state of stress in the plate only the in-plane stresses enter into the stress-strain relations, and we can write

$$\dot{\sigma}_{\alpha\beta} = \hat{L}_{\alpha\beta\gamma\delta}\dot{\eta}_{\gamma\delta} \tag{2.4}$$

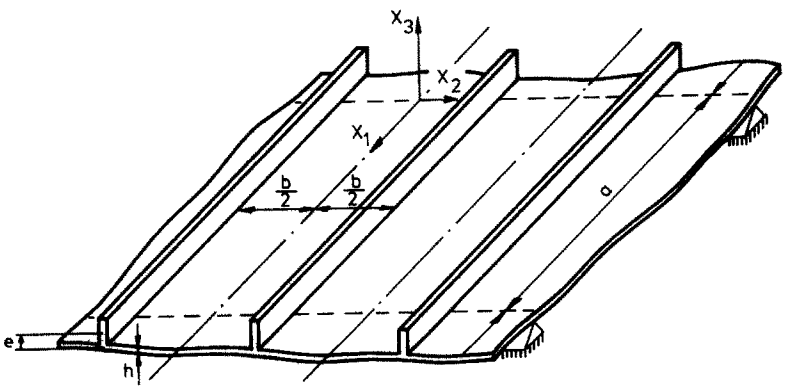

Fig. 1. Part of an integrally stiffened continuous panel on several transverse supports at distance a.

where the in-plane moduli are given by

$$\hat{L}_{\alpha\beta\gamma\delta} = L_{\alpha\beta\gamma\delta} - \frac{L_{\alpha\beta 33}L_{\gamma\delta 33}}{L_{3333}}. \tag{2.5}$$

The plate theory approximation to the strain increments at distance x_3 from the middle surface is

$$\dot{\eta}_{\alpha\beta} = \dot{\epsilon}_{\alpha\beta} - x_3\dot{\kappa}_{\alpha\beta}. \tag{2.6}$$

Using this and the usual definition of the membrane stress tensor $N_{\alpha\beta}$ and the moment tensor $M_{\alpha\beta}$, we find the incremental relations

$$\dot{N}_{\alpha\beta} = H^{(1)}_{\alpha\beta\gamma\delta}\dot{\epsilon}_{\gamma\delta} + H^{(2)}_{\alpha\beta\gamma\delta}\dot{\kappa}_{\gamma\delta}, \quad \dot{M}_{\alpha\beta} = H^{(2)}_{\alpha\beta\gamma\delta}\dot{\epsilon}_{\gamma\delta} + H^{(3)}_{\alpha\beta\gamma\delta}\dot{\kappa}_{\gamma\delta} \tag{2.7}$$

where

$$H^{(i)}_{\alpha\beta\gamma\delta} = \int_{-(h/2)}^{(h/2)} \hat{L}_{\alpha\beta\gamma\delta}(-x_3)^{i-1}\,\mathrm{d}x_3. \tag{2.8}$$

For the stiffeners we only account for plasticity due to uniaxial stresses σ_s parallel with the centre line. Then with the instantaneous uniaxial modulus $\hat{L}_s$, the incremental stress–strain relationship is

$$\dot{\sigma}_s = \hat{L}_s\dot{\eta}_s, \quad \dot{\eta}_s = \dot{\epsilon}_s - (x_3 - e)\dot{\kappa}_s. \tag{2.9}$$

The incremental relations for the axial stiffener force N_s and the bending moment M_s are

$$\dot{N}_s = H_s^{(1)}\dot{\epsilon}_s + H_s^{(2)}\dot{\kappa}_s, \quad \dot{M}_s = H_s^{(2)}\dot{\epsilon}_s + H_s^{(3)}\dot{\kappa}_s \tag{2.10}$$

where

$$H_s^{(i)} = b_s\int_{e-(h_s/2)}^{e+(h_s/2)} \hat{L}_s(e - x_3)^{i-1}\,\mathrm{d}x_3. \tag{2.11}$$

Here the height and the width of the stiffener are denoted h_s and b_s, respectively. The increment of twisting moment in a stiffener is taken to be given by the elastic expression

$$\dot{M}_{Vs} = G_sK_s\dot{w}_{,12}. \tag{2.12}$$

This approximation is made in order to avoid a full solution of the mixed compression-bending-twisting problem for the stiffeners in the plastic range. This does not mean any approximation in the case of buckling as a wide column, in which the stiffeners stay untwisted, and neither does it affect any bifurcation load based on a flow theory of plasticity with no corners on the yield surface. However, in computations of post-buckling behaviour or behaviour of imperfect panels, in which the stiffeners twist, equation (2.12) overestimates the torsional stiffness somewhat.

Small-strain J_2 flow-theory with isotropic hardening is used, where the J_2 invariant is defined as

$$J_2 = \frac{1}{2}s_{ij}s_{ij} \tag{2.13}$$

in terms of the stress deviator $s_{ij} = \sigma_{ij} - (1/3)\delta_{ij}\sigma_{kk}$. The instantaneous moduli of J_2 flow-theory are

$$L_{ijkl} = \frac{E}{1+\nu}\left\{\frac{1}{2}(\delta_{ik}\delta_{jl} + \delta_{il}\delta_{jk}) + \frac{\nu}{1-2\nu}\delta_{ij}\delta_{kl} - \frac{f s_{ij}s_{kl}}{1+\nu+2fJ_2}\right\} \tag{2.14}$$

where E and ν are Young's modulus and Poisson's ratio, respectively, and

$$f(J_2) = \begin{cases} \dfrac{3}{4J_2}\left(\dfrac{E}{E_t} - 1\right), & \text{for } J_2 = (J_2)_{\max} \text{ and } \dot{J}_2 \geq o \\ 0, & \text{for } J_2 < (J_2)_{\max} \text{ or } \dot{J}_2 < 0. \end{cases} \tag{2.15}$$

Here the tangent modulus E_t is the slope of a stress–strain curve for uniaxial tension. The particular uniaxial stress–strain curve chosen here is a power hardening law with a well defined yield stress σ_y and continuous tangent modulus

$$\dot{\epsilon} = \begin{cases} \dfrac{\dot{\sigma}}{E}, & \text{for } \sigma \leq \sigma_y \\ \dfrac{\sigma_y}{E}\left(\dfrac{1}{n}\left(\dfrac{\sigma}{\sigma_y}\right)^n - \dfrac{1}{n} + 1\right), & \text{for } \sigma > \sigma_y. \end{cases} \tag{2.16}$$

3. BIFURCATION BEHAVIOUR IN THE PLASTIC RANGE

The stress state in a perfect panel prior to bifurcation is a pure membrane state with the only nonvanishing stress component being a constant axial stress $\sigma_{11} = \lambda\sigma^0_{11}$ at every point of the plate and the stiffeners. Thus, in general the relationship between the in-plane stress rates and strain rates stops being isotropic as soon as the absolute value of $\lambda\sigma^0_{11}$ exceeds the yield stress σ_y. Then the lowest bifurcation load can be determined as that of an elastic stiffened orthotropic plate with moduli equal to the instantaneous plastic moduli.

In the following we use the expressions $E_1 = \hat{L}_{1111}$, $E_2 = \hat{L}_{2222}$, $E_{12} = \hat{L}_{1122}$, $E_G = \hat{L}_{1212}$ and $E_s = \hat{L}_s$ for the plastic branch of the nonvanishing components of instantaneous moduli in the prebuckling state at the bifurcation point. We also use the area A_s and the area moment of inertia I_s of the stiffener cross-section, and the expression $D_1 = E_1h^3/12$, $D_2 = E_2h^3/12$, $D_{12} = E_{12}h^3/12$ and $D_G = E_Gh^3/6$. Then by application of the equilibrium conditions for the panel in terms of $N_{\alpha\beta}$, $M_{\alpha\beta}$, N_s, M_s and w that have been derived from the principle of virtual work[4], we find the following linear buckling equations for the buckling mode (u_1, u_2, w) and the critical load parameter λ_c

$$E_1u_{1,11} + E_Gu_{1,22} + (E_{12} + E_G)u_{2,12} = 0 \tag{3.1}$$

$$(E_{12} + E_G)u_{1,12} + E_Gu_{2,11} + E_2u_{2,22} = 0 \tag{3.2}$$

$$D_1w_{,1111} + 2(D_{12} + D_G)w_{,1122} + D_2w_{,2222} - \lambda_cN^0_{11}w_{,11} = 0 \tag{3.3}$$

and the corresponding linear discontinuity conditions at a stiffener

$$-E_Gh(u^+_{1,2} - u^-_{1,2} + u^+_{2,1} - u^-_{2,1}) - E_sA_s(u^-_{1,11} - ew^-_{,111}) = 0 \tag{3.4}$$

$$-E_2(u^+_{2,2} - u^-_{2,2}) - E_{12}(u^+_{1,1} - u^-_{1,1}) = 0 \tag{3.5}$$

$$D_2(w^+_{,222} - w^-_{,222}) + E_sI_sw^-_{,1111} - eE_sA_s(u^-_{1,111} - ew^-_{,1111}) - \lambda_c N_s^0 w^-_{,11} = 0 \tag{3.6}$$

$$-D_2(w^+_{,22} - w^-_{,22}) - G_sK_sw^-_{,112} - \lambda_c e^2 N_s^0 w^-_{,112} = 0 \tag{3.7}$$

$$u_1^+ = u_1^-, \quad u_2^+ = u_2^-, \quad w^+ = w^-, \quad w^+_{,2} = w^-_{,2}. \tag{3.8}$$

Here superscript + refers to the side of the stiffener in the positive x_2-direction and superscript − refers to the other side. The prebuckling unit membrane stress and stiffener force are $N^0_{11} = \sigma^0_{11}h$ and $N_s^0 = \sigma^0_{11}A_s$, respectively.

For the panel of finite length in the x_1-direction the simple support boundary conditions at the edges $x_1 = 0$, a are taken to be

$$u_{1,1} = u_2 = w = w_{,11} = 0. \tag{3.9}$$

Here the condition $u_2 = 0$ gives a slight overestimation of some bifurcation loads for a panel that is really free to slide tangentially along the simply supported edges. For the continuous panel over several transverse supports at distance a (Fig. 1) the bifurcation load and the bifurcation mode between two supports are identical with the solution of equations (3.1)–(3.9).

In the infinitely wide periodic structure, the buckling mode displacements u_1 and w are symmetric about the centre line $x_2 = 0$ between two stiffeners, and u_2 is antisymmetric about this line. After rather lengthy calculations we find that the solution of equations (3.1)–(3.9) take the form

$$w = \{c_1 \cosh(r_1x_2) + c_2 \cos(r_2x_2)\} \sin\frac{k\pi x_1}{a} \tag{3.10}$$

$$u_1 = \{c_3 \cosh(r_3x_2)\cos(r_4x_2) + c_4 \sinh(r_3x_2)\sin(r_4x_2)\} \cos\frac{k\pi x_1}{a} \tag{3.11}$$

$$u_2 = \{(c_3b_1 + c_4b_2)\sinh(r_3x_2)\cos(r_4x_2) + (-c_3b_2 + c_4b_1)\cosh(r_3x_2)\sin(r_4x_2)\} \sin\frac{k\pi x_1}{a} \tag{3.12}$$

in which k is a positive integer, and the constants r_1, r_2, r_3, r_4, b_1 and b_2 depend on k, a, λ_c and the instantaneous moduli. The expressions for these parameters are lengthy and will not be given here. In the special case of isotropy, treated in [4], r_4 equals zero and the expressions (3.11) and (3.12) are replaced by different expressions.

The same mode expressions (3.10)–(3.12) apply in the local coordinate system of a neighbouring plate section between two stiffeners, but with different constants $c_5 - c_8$ instead of $c_1 - c_4$. Substituting these buckling mode expressions in the discontinuity conditions (3.4)–(3.8), we obtain eight linear, homogeneous equations for the constants $c_1 - c_8$. An iterative procedure is used to determine the smallest critical bifurcation load λ_c and the corresponding instantaneous moduli, for which the determinant of the coefficient matrix vanishes.

Buckling as a wide Euler column, with $k = 1$ and identical modes for all plate sections between two stiffeners, is critical as long as the stiffeners are relatively weak. When the bending stiffness of the stiffeners is sufficiently high, local buckling of the plate between the stiffeners

occurs first, usually with a value of k somewhat above a/b. The local buckling displacement fields in two neighbouring plate sections are usually identical with opposite sign. However, in cases of relatively large torsional stiffness of the stringers, the mode shapes are identical for all plate sections between two stiffeners.

For some panels specified by $a/b = 4$, $e/b = 0{\cdot}1$, $(A_s + h.b)/b^2 = 0{\cdot}0256$, and with integral stiffeners of rectangular cross-section, bifurcation loads are given in Fig. 2. The ratio $\alpha = (1 + A_s/bh)^{-1}$ between the amount of material in the plate and that in the whole panel is chosen as a design parameter. The plastic bifurcation loads are given for different ratios of yield stress and Young's modulus, and in all cases the strain hardening parameter $n = 10$ has been chosen. Figure 2 also compares the bifurcation loads predicted by J_2 flow theory with results of J_2 deformation theory. For the wide column buckling mode these results are indistinguishable from one another, and for the local buckling mode there is only a minor difference in our range of interest.

4. PLASTIC POST-BIFURCATION BEHAVIOUR

An asymptotic theory of the post-bifurcation behaviour of structures in the plastic range has been developed by Hutchinson [11, 12], which extends the bifurcation analysis of Hill [13, 14] into the initial post-bifurcation range. In the vicinity of the bifurcation point the load is expanded in terms of the buckling mode displacement amplitude, as is done in Koiter's theory for elastic post-buckling behaviour [15]. However, in the plastic range elastic unloading plays a crucial role after bifurcation. In the present paper we shall use the specialization to Donnell–Mushtari–Vlasov theory of plates and shells given in [12].

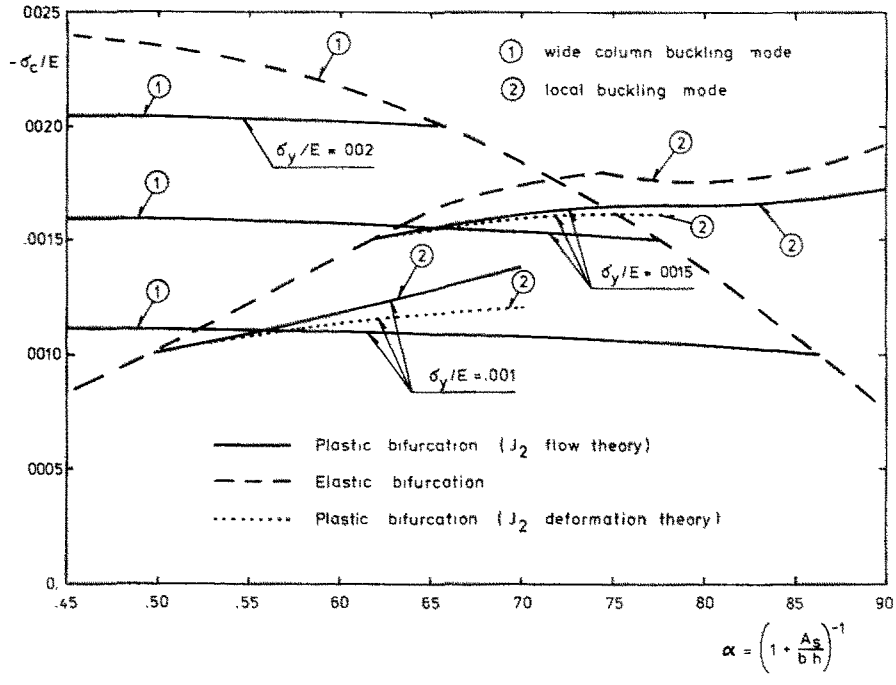

Fig. 2. Bifurcation stress for panels specified by $a/b = 4$, $e/b = 0{\cdot}1$, $(A_s + hb)/b^2 = 0{\cdot}0256$ and $\nu = 0{\cdot}3$. All plastic bifurcation loads are taken for a strain hardening parameter $n = 10$.

An asymptotically exact expression for the load parameter λ in terms of the amplitude ξ of the buckling mode displacement is obtained of the form

$$\lambda = \lambda_c + \lambda_1 \xi + \lambda_2 \xi^{1+\beta} + \dots \tag{4.1}$$

for $\xi \geqslant 0$. For mode displacements in the opposite direction, we change the sign of ξ, and then expression (4.1) still applies with different constants λ_1, λ_2 and β. The buckling mode is normalized so that for $\xi = 1$ the maximum deflection w is equal to the plate thickness.

The constant λ_1 is determined from the Shanley condition, such that when the buckling mode starts to grow, plastic loading occurs everywhere in the current plastic zone, except in at least one point where neutral loading takes place. This is true in general, except for cases in which a larger initial slope λ_1 would be predicted by the non-linear hypo-elastic comparison problem obtained by neglecting the possibility of elastic unloading. The initial post-bifurcation slope for this hype-elastic problem is given by the expression[12]

$$\lambda_1^{he} = -\frac{\mathscr{A}}{\mathscr{B}} \tag{4.2}$$

where for the integrally stiffened panel simply supported at the two edges $x_1 = 0, a$

$$\begin{aligned}\mathscr{A} = &\int_0^a \int_0^b 3\overset{(1)}{N}_{\alpha\beta}\overset{(1)}{w}_{,\alpha}\overset{(1)}{w}_{,\beta}\,dx_2\,dx_1 + \int_0^a 3\overset{(1)}{N}_s(\overset{(1)}{w}_{,1}\overset{(1)}{w}_{,1} \\ &+ e^2\overset{(1)}{w}_{,12}\overset{(1)}{w}_{,12})\,dx_1 + \int_0^a \int_0^b \int_{-(h/2)}^{(h/2)} \overset{(1)}{\sigma}_{\mu\nu}\left.\frac{\partial \hat{L}_{\alpha\beta\gamma\delta}}{\partial \sigma_{\mu\nu}}\right|_c \overset{(1)}{\eta}_{\alpha\beta}\overset{(1)}{\eta}_{\gamma\delta}\,dx_3\,dx_2\,dx_1 \\ &+ b_s\int_0^a \int_{e-(h_s/2)}^{e+(h_s/2)} \overset{(1)}{\sigma}_s\left.\frac{\partial \hat{L}_s}{\partial \sigma_s}\right|_c \overset{(1)}{\eta}_s\overset{(1)}{\eta}_s\,dx_3\,dx_1\end{aligned} \tag{4.3}$$

$$\begin{aligned}\mathscr{B} = &\int_0^a \int_0^b 2\left.\frac{\partial \overset{(0)}{N}_{\alpha\beta}}{\partial\lambda}\right|_c \overset{(1)}{w}_{,\alpha}\overset{(1)}{w}_{,\beta}\,dx_2\,dx_1 + \int_0^a 2\left.\frac{\partial \overset{(0)}{N}_s}{\partial\lambda}\right|_c (\overset{(1)}{w}_{,1}\overset{(1)}{w}_{,1} \\ &+ e^2\overset{(1)}{w}_{,12}\overset{(1)}{w}_{,12})\,dx_1 + \int_0^a \int_0^b \int_{-(h/2)}^{(h/2)} \left(\left.\frac{\partial \overset{(0)}{\sigma}_{\mu\nu}}{\partial\lambda}\right|_c \left.\frac{\partial \hat{L}_{\alpha\beta\gamma\delta}}{\partial \sigma_{\mu\nu}}\right|_c \overset{(1)}{\eta}_{\alpha\beta}\overset{(1)}{\eta}_{\gamma\delta}\right. \\ &\left. + \overset{(1)}{\sigma}_{\mu\nu}\left.\frac{\partial \hat{L}_{\alpha\beta\gamma\delta}}{\partial \sigma_{\mu\nu}}\right|_c \left.\frac{\partial \overset{(0)}{\eta}_{\alpha\beta}}{\partial\lambda}\right|_c \overset{(1)}{\eta}_{\gamma\delta}\right) dx_3\,dx_2\,dx_1 \\ &+ b_s\int_0^a \int_{e-(h_s/2)}^{e+(h_s/2)} \left(\left.\frac{\partial \overset{(0)}{\sigma}_s}{\partial\lambda}\right|_c \left.\frac{\partial \hat{L}_s}{\partial\lambda}\right|_c \overset{(1)}{\eta}_s\overset{(1)}{\eta}_s + \overset{(1)}{\sigma}_s\left.\frac{\partial \hat{L}_s}{\partial \sigma_s}\right|_c \left.\frac{\partial \overset{(0)}{\eta}_s}{\partial\lambda}\right|_c \overset{(1)}{\eta}_s\right) dx_3\,dx_1.\end{aligned} \tag{4.4}$$

For the continuous panel on several transverse supports the integrations must be taken over two bays from 0 to $2a$ in the x_1-direction. The pre-buckling solution and the buckling mode are indicated by (0) and (1), respectively, above the quantities, and subscript c indicates a quantity evaluated at the bifurcation point. Quantities associated with the stiffener are evaluated at $x_2 = b/2$. If a case is found for which $\lambda_1^{he} > \lambda_1$, equation (4.1) must be replaced by $\lambda = \lambda_c + \lambda_1^{he}\xi + 0(\xi^2)$, and no elastic unloading occurs immediately after bifurcation.

The constant β is determined from the lowest order terms in a Taylor expansion of the shape of the elastic unloading zone together with an asymptotic expansion of the principle of virtual work [12]. Finally λ_2 is determined from the lowest order terms in this expansion of the principle of virtual work

$$\{-\lambda_2(1+\beta)\}^{1/\beta} C \int_{\overset{*}{V}} f(\overset{*}{z}_i)\, \mathrm{d}\overset{*}{V} = \mathscr{A} + \lambda_1 \mathscr{B} \tag{4.5}$$

where C is a negative constant involving known quantities. In all cases we find $0 < \beta < 1$, $\lambda_1 > 0$ and $\lambda_2 < 0$. The instantaneous elastic unloading region is denoted by $\overset{*}{V}$ and the equation of the instantaneous neutral loading surface enclosing $\overset{*}{V}$ is given by $f(\overset{*}{z}_i) = 0$. Stretched boundary-layer coordinates $\overset{*}{z}_i$ are chosen such that the surface (surfaces) enclosing $\overset{*}{V}$ are independent of ξ to lowest order when written in terms of $\overset{*}{z}_i$.

As an example we shall give some detailed expressions for the special case of a panel on two supports at wide column mode bifurcation in negative x_3-direction, in which the wedge shape of the neutral loading surface, shown in Fig. 3c below, differs from the shapes discussed in [12]. Here the stretched coordinates are given by the expressions

$$\overset{*}{z}_1 = \frac{\xi^{-\beta/2} z_1}{\{-(1+\beta)\lambda_2\}^{1/2}}, \quad \overset{*}{z}_2 = \frac{\xi^{-\beta} z_2}{-(1+\beta)\lambda_2}, \quad \overset{*}{z}_3 = \frac{\xi^{-\beta} z_3}{-(1+\beta)\lambda_2} \tag{4.6}$$

in terms of local Cartesian coordinates z_i centered at the surface point in which elastic unloading starts, with z_3 directed along the outward surface normal and z_1 parallel with a stiffener. For this case $f(\overset{*}{z}_i)$ takes the form

$$f(\overset{*}{z}_i) = C_0 - C_3 \overset{*}{z}_3 \mp C_2 \overset{*}{z}_2 - C_{11} \overset{*}{z}_1{}^2, \quad \text{for} \quad \overset{*}{z} \gtrless 0 \tag{4.7}$$

in which C_3 is negative while the other constants are positive.

For the panel simply supported at the two edges $x_1 = 0, a$, Fig. 3 indicates the shape of the elastic unloading zones that propagate into the material for the case of local buckling and also for the case of wide column buckling either in the positive x_3-direction or in the negative x_3-direction. Figure 3 also gives the corresponding values of β. For the continuous panel on several transverse supports at distance a, the shape of the elastic unloading zones at local buckling are identical with Fig. 3a. When the continuous panel bifurcates in the wide column buckling mode the unloading zones shown in Fig. 3b appear in half of the bays that buckle in positive x_3-direction whereas no

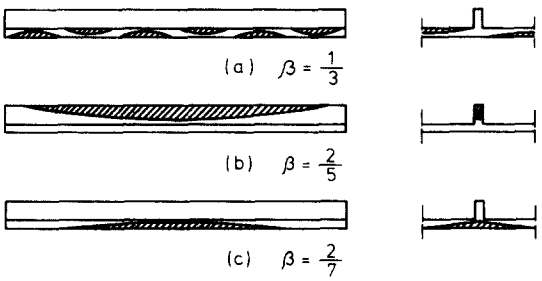

Fig. 3. Shape of elastic unloading zones in panel simply supported at the two edges (plate thickness exaggerated). (a) Local buckling with 6 half sine waves in x_1-direction. (b) Wide column buckling in positive x_3-direction. (c) Wide column buckling in negative x_3-direction.

elastic unloading occurs at bifurcation in the other half of the bays that buckle in negative x_3-direction.

Figure 4 shows the asymptotic relationship between load and mode displacement amplitude for wide column mode bifurcation in a panel simply supported at the two edges, for wide column mode bifurcation in a continuous panel on several transverse supports and for local mode bifurcation in a panel with either of these two sets of boundary conditions. The design parameter α relates to Fig. 2. More detailed information about the constants in (4.1) are given in Table 1 for various panel designs. The table also gives the maximum load parameter λ_{max} according to the truncated expansion (4.1) and the corresponding mode deflection amplitude ξ_{max}, where

$$\xi_{max} = \left(-\frac{\lambda_1}{\lambda_2(1+\beta)}\right)^{1/\beta}, \quad \lambda_{max} = \lambda(\xi_{max}). \tag{4.8}$$

For bifurcation in the local buckling mode the plastic post-bifurcation behaviour is symmetric, and the same is true for wide column mode bifurcation of the continuous panel. At

Table 1. Constants in asymptotic expansion for various panel designs with $a/b = 4$, $e/b = 0{\cdot}1$, $(A_s + hb)/b^2 = 0{\cdot}0256$ and $\nu = 0{\cdot}3$. A and B denote wide column mode bifurcation in positive and in negative x_3-direction, respectively, for panel supported on the two edges, C denotes column mode bifurcation for continuous panel and D denotes local mode bifurcation

α	σ_c/σ_y	σ_y/E	n	λ_1^{he}/λ_c	λ_1/λ_c	λ_2/λ_c	β	λ_{max}/λ_c	ξ_{max}	
				0·173	0·745	−1·291	2/5	1·02320	0·1090	*A*
0·650	1·081	0·0010	10	−0·173	0·186	−0·475	2/7	1·00064	0·0155	*B*
				0·0	0·745	−1·893	2/5	1·00891	0·0419	*C*
0·525	1·044	0·0010	10	0·0	1·008	−3·767	1/3	1·00204	0·0081	*D*
				0·212	0·925	−3·242	2/5	1·00496	0·0188	*A*
0·700	1·023	0·0015	10	−0·212	0·244	−1·044	2/7	1·00014	0·0026	*B*
				0·0	0·925	−4·746	2/5	1·00191	0·0072	*C*
0·640	1·021	0·0015	10	0·0	1·273	−6·535	1/3	1·00099	0·0031	*D*
				0·135	0·744	−1·036	2/5	1·04009	0·1885	*A*
0·650	1·211	0·0010	4	−0·135	0·196	−0·408	2/7	1·00139	0·0318	*B*
				0·0	0·744	−1·482	2/5	1·01641	0·0772	*C*

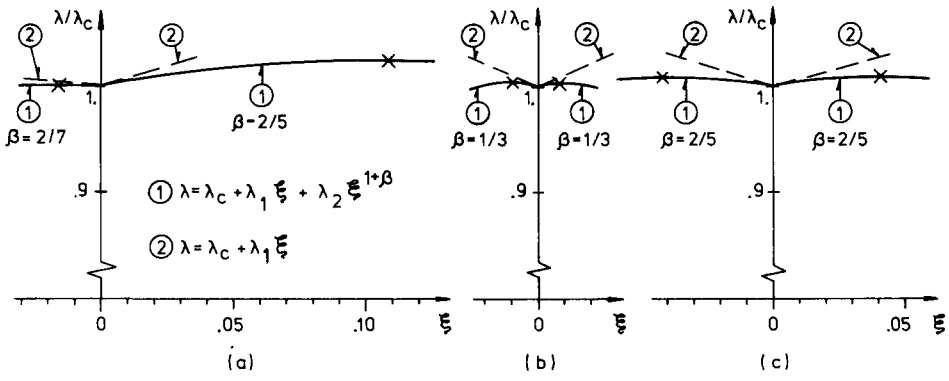

Fig. 4. Load-mode displacement relationship. (a) Wide column buckling in panel simply supported at the two edges. Buckling in positive x_3-direction for positive ξ ($\alpha = 0{\cdot}65$, $\sigma_y/E = 0{\cdot}001$, $n = 10$). (b) Local buckling ($\alpha = 0{\cdot}525$, $\sigma_y/E = 0{\cdot}001$, $n = 10$). (c) Wide column buckling for continuous panel on several transverse supports ($\alpha = 0{\cdot}65$, $\sigma_y/E = 0{\cdot}001$, $n = 10$).

wide column mode bifurcation for a panel simply supported at the two edges the post-bifurcation behaviour is asymmetric as shown in Fig. 4a and in Table 1. The lowest carrying capacity is for mode displacements in the negative x_3-direction contrary to the asymmetry for the linearly elastic panel. This is due to the dominance of material nonlinearities over geometric nonlinearities in the expressions (4.3) and (4.4) for $\mathscr{A}$ and $\mathscr{B}$ and to the relatively smaller values of both λ_1 and β for mode deflections in the negative x_3-direction.

The asymptotic analysis is not used here to treat cases of two coincident plastic bifurcation loads. However, in [10] a numerical computation of the post-bifurcation behaviour is shown for such a case.

Two of the most interesting results of the asymptotic post-bifurcation analysis that are confirmed by the numerical calculations below are the strongly asymmetric behaviour at wide column mode bifurcation for the panel on two supports, with the lowest load carrying capacity for negative mode deflections, and the fact that the continuous panel at column mode bifurcation has a load carrying capacity between the two extremes for the panel on two supports.

5. NUMERICAL METHOD FOR IMPERFECT PANEL

An initial imperfection is specified and the behaviour of an imperfect panel is determined by the following incremental procedure. At each stage of the loading history, the normal deflection w, and the membrane forces $N_{\alpha\beta}$ and N_s are known. Incremental equilibrium is expressed in terms of the following variational principle: Among all displacement increment fields that satisfy the kinematical boundary conditions, the actual displacement increments satisfy

$$\delta I = 0 \tag{5.1a}$$

where, for the panel simply supported at the edges $x_1 = 0, a$

$$\begin{aligned} I = \frac{1}{2}\int_0^a \int_0^b & [H^{(1)}_{\alpha\beta\gamma\delta}\dot{\epsilon}_{\alpha\beta}\dot{\epsilon}_{\gamma\delta} + 2H^{(2)}_{\alpha\beta\gamma\delta}\dot{\epsilon}_{\alpha\beta}\dot{\kappa}_{\gamma\delta} \\ & + H^{(3)}_{\alpha\beta\gamma\delta}\dot{\kappa}_{\alpha\beta}\dot{\kappa}_{\gamma\delta} + N_{\alpha\beta}\dot{w}_{,\alpha}\dot{w}_{,\beta}]\,\mathrm{d}x_1\,\mathrm{d}x_2 + \frac{1}{2}\int_0^a [H_s^{(1)}\dot{\epsilon}_s\dot{\epsilon}_s \\ & + 2H_s^{(2)}\dot{\epsilon}_s\dot{\kappa}_s + H_s^{(3)}\dot{\kappa}_s\dot{\kappa}_s + G_sK_s\dot{w}^2_{,12} + N_s(\dot{w}^2_{,1} + e^2\dot{w}^2_{,12})]\,\mathrm{d}x_1 \\ & - \dot{\lambda}\left[\int_0^b N^0_{11}\dot{u}_1\,\mathrm{d}x_2 + N_s^0(\dot{u}_1 - e\dot{w}_{,1})\right]_0^a. \end{aligned} \tag{5.1b}$$

For the continuous panel the integrations in equation (5.1b) must be taken over one whole period in the x_1-direction. Quantities associated with the stiffener are evaluated at $x_2 = b/2$, $\dot{\lambda}$ is the prescribed increment of the load parameter, the moduli $H^{(i)}_{\alpha\beta\gamma\delta}$ and $H_s^{(i)}$ are defined by (2.8) and (2.11), respectively, and the incremental strain quantities are given in terms of the displacements by (2.1) and (2.2).

An approximate solution of (5.1) is obtained by a combined Rayleigh Ritz-finite element procedure due to Kawai and Ohtsubo [16, 17] and first employed in an elastic–plastic analysis by Ohtsubo [18]. The increment of normal displacement $\dot{w}$, is expanded in terms of smooth functions as in the standard Rayleigh Ritz method,

$$\dot{w} = \sum_{J=1}^{N} \dot{\xi}^*_J \hat{w}^J \tag{5.2}$$

where the $\hat{w}^j$ are the assumed functions for the Rayleigh Ritz solution. The in-plane displacements $\hat{u}_\alpha$ are determined by a finite element calculation. In the calculation, the plate is divided into rectangular elements and the functions $\hat{u}_\alpha$ are expanded in terms of cubic "serendipity" functions[19]. Along the stiffener these functions reduce to Lagrangian cubics.

Solving first equation (5.1a) for the in-plane displacements, we find a displacement field $\hat{u}_\alpha{}^j$ corresponding to each $\hat{w}^j$. In addition we use the finite element method to find two pure in-plane modes $\hat{u}_\alpha{}^{N+1}$ and $\hat{u}_\alpha{}^{N+2}$, so that the in-plane displacement functions are given by

$$\dot{u}_\alpha = \sum_{j=1}^{N+2} \dot{\xi}_j^* \hat{u}_\alpha{}^j. \tag{5.3}$$

Equations (5.2) and (5.3) now give the trial functions employed in the Rayleigh Ritz procedure for a panel.

For the numerical computation of the behaviour of continuous panels on several transverse supports we restrict ourselves to panels in which the deformation pattern is symmetric about any centre line $x_1 = (a/2)$ between two supports (Fig. 1), so that we need only consider the region $-(a/2) \leq x_1 \leq (a/2)$, $0 \leq x_2 \leq b$. For the smooth out-of-plane functions $\hat{w}_j$ we choose the wide column buckling mode, the local buckling mode with the smallest buckling stress corresponding to an odd wave number k, and a mode with $k = 1$ that is able to relatively decrease or increase the bulging of the plate between the stiffeners in the wide column buckling mode. Furthermore, we choose the local buckling mode multiplied by $\sin(\pi x_1/a)$ and the wide column buckling mode multiplied by $\sin(\pi x_1/a)$ thus being able to vary the relative amounts introduced of these two buckling modes in two neighbouring bays. In addition to these five $\hat{w}^j$ modes some others have been tried without finding any that had an appreciable effect.

For the continuous panel the finite element computation of an in-plane displacement field $\hat{u}_\alpha{}^j$ corresponding to $\hat{w}^j$ is carried out with $\hat{u}_2{}^j = 0$ at $x_2 = 0, b$ and $\hat{u}_1{}^j = 0$ at $x_1 = -(a/2), (a/2)$. The additional in-plane mode $\hat{u}_\alpha{}^{N+1}$ is computed with $\hat{u}_2{}^{N+1} = 0$ at $x_2 = 0, b$ and prescribed uniform displacements $\hat{u}_1{}^{N+1}$ at $x_1 = -(a/2), (a/2)$. The mode $\hat{u}_\alpha{}^{N+2}$ is computed with $\hat{u}_2{}^{N+2} = 0$ at $x_1 = -(a/2), (a/2)$ and prescribed uniform displacements $\hat{u}_2{}^{N+2}$ at $x_2 = 0, b$.

For the panel on two simple supports at the edges $x_1 = 0, a$ the smooth out-of-plane functions nearly identical with the four first $\hat{w}^j$ described above and the in-plane boundary conditions are given precisely in[10].

In the solution of the Rayleigh Ritz problem, we avoid difficulties around the maximum load by always prescribing that of the $N+3$ parameters $\dot{\xi}_1^*, \dot{\xi}_2^*, \ldots, \dot{\xi}_{N+2}^*, \dot{\lambda}$ that is numerically largest in the previous increment, and then solving (5.1a) for the remaining $N+2$ parameters.

Once $\dot{\xi}_j^*$ have been determined by the Rayleigh Ritz method, corrected mode amplitude increments $\dot{\xi}_j$ are found by also using the curvatures of the functions $\xi_j(\lambda)$. These curvatures are estimated numerically using the slopes of the previous increment[20]. Comparison with more precise solutions by the Newton–Raphson method for an elastic panel[5] has demonstrated that this quadratic incremental method is far more efficient than the straightforward linear incremental method.

The numerical integration scheme employed in both the finite element and Rayleigh Ritz parts of the calculations is as follows. The area integral in (5.1b) is evaluated by 16 point (4×4) Gaussian quadrature in each element while the line integral along the stiffener is evaluated by 4 point Gaussian quadrature in each element. The integrals through the thickness are evaluated by Simpsons rule, with 7 points employed in (2.8) and (2.11).

In order to evaluate (5.1b) it is necessary to know the current values of the moduli $H^{(i)}_{\alpha\beta\gamma\delta}$ and

$H_s^{(i)}$. Therefore, the active branches of the moduli $\hat{L}_{\alpha\beta\gamma\delta}$ and $\hat{L}_s$ are evaluated at each integration point. If the stress state at an integration point is on its current yield surface, the plastic branch is taken to be active. If $\dot{J}_2$ for that integration point turns out to be negative, the elastic branch is taken to be active in the next loading increment. This procedure is only accurate if small increments are used and if the transition from loading to unloading, or vice versa, occurs only once or twice during the loading history.

After experiments with various numbers of the rectangular cubic "serendipity" elements it was found that for the panel dimensions considered a good solution is obtained by dividing the region $-(a/2) \leq x_1 \leq (a/2), 0 \leq x_2 \leq b$ for the continuous panel or the region $0 \leq x_1 \leq a, 0 \leq x_2 \leq b$ for the panel simply supported on the two edges into 12 elements in the x_1-direction and 2 elements in the x_2-direction.

The combined Rayleigh Ritz-finite element method described here differs in several respects from that employed by Ohtsubo[18]. In the present paper the plastic strains are accounted for by the incremental stiffness or tangent modulus method rather than by the initial strain method, and furthermore no *a priori* assumption is made concerning the distribution of plastic strains through the thickness. Also, the effect of strain hardening in included.

The computational advantage of the combined Rayleigh Ritz-finite element method versus a full finite element calculation is that it eliminates the necessity of direct coupling of in-plane and out-of-plane nodal degrees of freedom, thus reducing the size and the bandwidth of the finite element equations.

In addition to the combined Rayleigh Ritz-finite element solution a few cases of a panel simply supported at the two edges, were computed by a full Rayleigh Ritz method. Here, apart from the bifurcation modes the in-plane trial functions taken in terms of trigonometric functions were based on a general knowledge of the shape of the displacement fields growing with the square of each of the two bifurcation mode amplitudes and with the product of these two amplitudes in elastic post-buckling. To obtain the same results as with the combined method, 27 trial functions and nearly twice the computer time were needed. Usually it is much more difficult to guess good in-plane trial functions than it is to guess good out-of-plane trial functions, and this makes the combined Rayleigh Ritz-finite element method very attractive.

6. BEHAVIOUR OF IMPERFECT PANELS

For some panels for which the bifurcation loads are specified in Fig. 2, the behaviour due to various imperfections is shown in Figs. 5–11. The first four figures describe panels simply supported on the two edges at distance a and the last three figures describe continuous panels on several transverse supports. Initial imperfections are considered in the shape of the wide column buckling mode and the local buckling mode, and the ratios between their amplitudes and the plate thickness are denoted $\bar{\xi}_w$ and $\bar{\xi}_l$, respectively. In the following ξ_w and ξ_l denote the additional growth of these two modes, and in the figures we only show the relationship between ξ_w and the load parameter λ.

The behaviour of some simply supported panels that bifurcate in the plastic range has been computed in[10], and there it was found that initial imperfections lowered the maximum carrying capacity in all cases considered. A few of these results are repeated in Fig. 5 to show the agreement between the numerically computed asymmetric post-bifurcation behaviour and the asymptotic results shown in Fig. 4a. The curves marked "perfect" in Figs. 5, 6, 9, 10 are actually the results of a numerical computation for panels with very small initial imperfections. Figure 5 also shows the strong sensitivity to negative wide column imperfections, explained by the

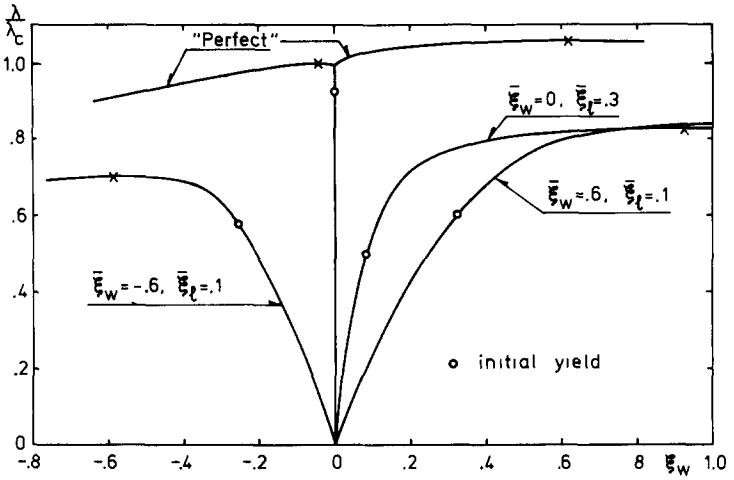

Fig. 5. Load vs wide column mode displacement for panel supported at the two edges that bifurcates plastically in wide column buckling mode ($\sigma_y/E = 0{\cdot}001$, $n = 10$, $\alpha = 0{\cdot}65$, $a/b = 4$, $e/b = 0{\cdot}1$, $(A_s + hb)/b^2 = 0{\cdot}0256$, $\nu = 0{\cdot}3$).

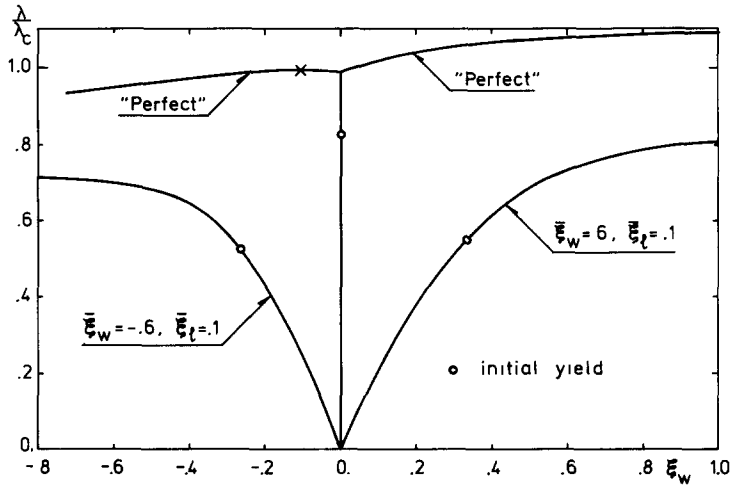

Fig. 6. Load vs wide column mode displacement for panel supported at the two edges that bifurcates plastically in wide column buckling mode ($\sigma_y/E = 0{\cdot}001$, $n = 4$, $\alpha = 0{\cdot}65$, $a/b = 4$, $e/b = 0{\cdot}1$, $(A_s + hb)/b^2 = 0{\cdot}0256$, $\nu = 0{\cdot}3$).

asymmetric post-bifurcation behaviour, and the sensitivity to positive wide column imperfections mainly due to interaction with the local buckling mode.

In Fig. 6 the same panel is considered with the strain hardening parameter changed to $n = 4$. Here bifurcation of the perfect structure occurs at stresses somewhat higher above the yield stress than in Fig. 5, but otherwise the behaviour exhibited in Fig. 6 only differs little from that in Fig. 5. However, at the smaller value of n the maxima occur at relatively larger mode amplitudes, as was also predicted by the asymptotic results in Table 1.

Figures 7 and 8 illustrate the effect of plasticity on panels on two simple supports that

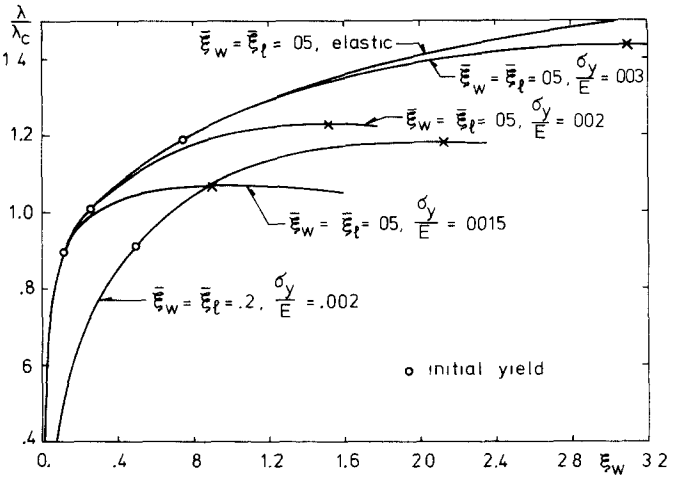

Fig. 7. Load vs wide column mode displacement for panel supported at the two edges that bifurcates elastically in local buckling mode ($\sigma_c/E = 0{\cdot}00112$, $n = 10$, $\alpha = 0{\cdot}525$, $a/b = 4$, $e/b = 0{\cdot}1$, $(A_s + hb)/b^2 = 0{\cdot}0256$, $\nu = 0{\cdot}3$).

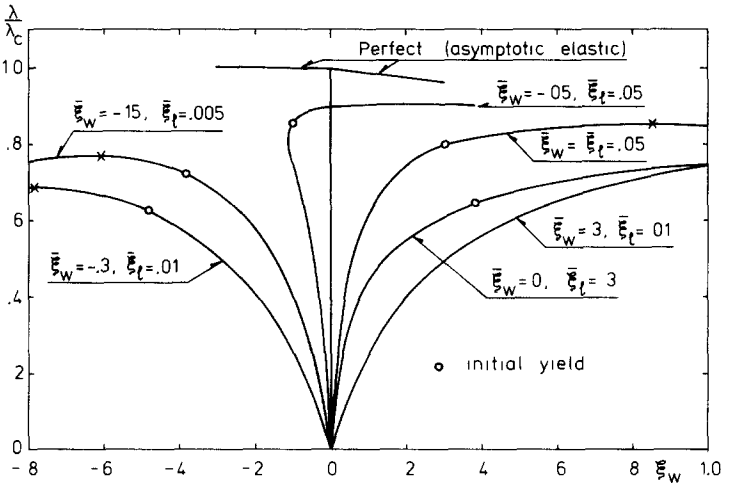

Fig. 8. Load vs wide column mode displacement for panel supported at the two edges with simultaneous elastic bifurcation in wide column and local buckling modes ($\sigma_y/E = 0{\cdot}00195$, $\sigma_c/\sigma_y = 0{\cdot}909$, $n = 10$, $\alpha = 0{\cdot}7165$, $a/b = 4$, $e/b = 0{\cdot}1$, $(A_s + hb)/b^2 = 0{\cdot}0256$, $\nu = 0{\cdot}3$).

bifurcate in the elastic range. For the panel in Fig. 7 that bifurcates elastically in the local buckling mode, the elastic theory predicts a maximum carrying capacity about 1·75 times the critical stress, occurring at a wide column mode displacement several times the plate thickness. The figure shows that this carrying capacity is considerably reduced for various levels of yield stress and that even for a yield stress nearly three times the bifurcation stress, the panel starts to yield just above the bifurcation load.

The panel described in Fig. 8 is designed so that elastic bifurcation occurs simultaneously in the wide column buckling mode and in the local buckling mode. According to linearly elastic theory such a design is more imperfection-sensitive than other designs due to a strong interaction between the two critical bifurcation modes. In Fig. 8 is shown the elastic asymptotic

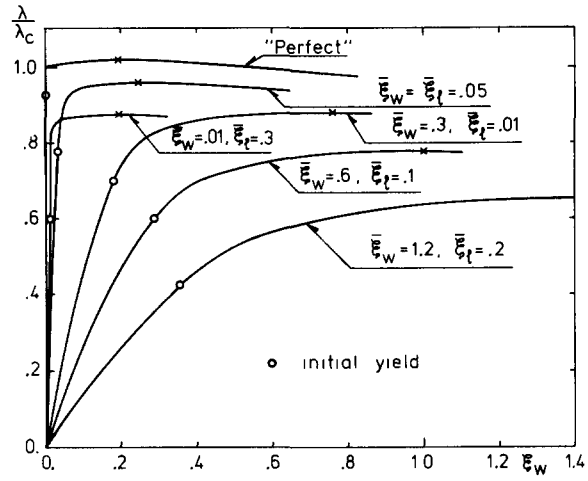

Fig. 9. Load vs wide column mode displacement for continuous panel on multiple supports that bifurcates plastically in wide column buckling mode ($\sigma_y/E = 0{\cdot}001$, $n = 10$, $\alpha = 0{\cdot}65$, $a/b = 4$, $e/b = 0{\cdot}1$, $(A_s + hb)/b^2 = 0{\cdot}0256$, $\nu = 0{\cdot}3$).

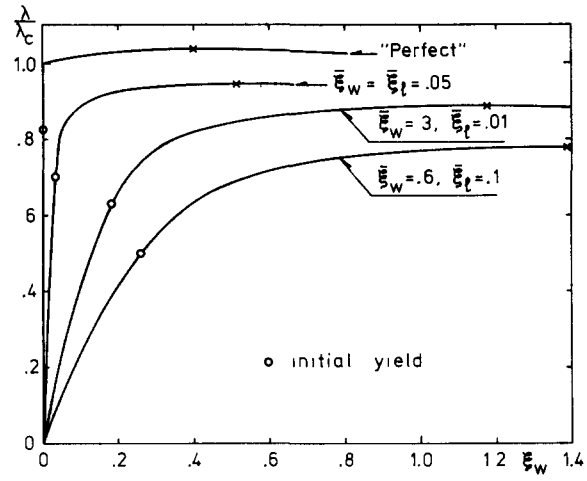

Fig. 10. Load vs wide column mode displacement for continuous panel on multiple supports that bifurcates plastically in wide column buckling mode ($\sigma_y/E = 0{\cdot}001$, $n = 4$, $\alpha = 0{\cdot}65$, $a/b = 4$, $e/b = 0{\cdot}1$, $(A_s + hb)/b^2 = 0{\cdot}0256$, $\nu = 0{\cdot}3$).

post-bifurcation behaviour computed according to [4], for which negative growth of ξ_w corresponds to $\xi_l = 0$ while positive growth of ξ_w occurs simultaneously with a growth of ξ_l. This elastic post-bifurcation behaviour clearly indicates the sensitivity to combinations of $\bar{\xi}_w$ and $\bar{\xi}_l$ that finally result in a positive growth of ξ_w. However, the computations with a yield stress 1·10 times the bifurcation stress show that plastic yielding makes the panel very sensitive to negative $\bar{\xi}_w$, as was the case in Fig. 5. Also for the case of positive column mode displacements plasticity adds to the imperfection-sensitivity.

For elastic continuous panels on several transverse supports Koiter and Pignataro[6] have shown that the imperfection-sensitivity found for panels on only two supports is somewhat

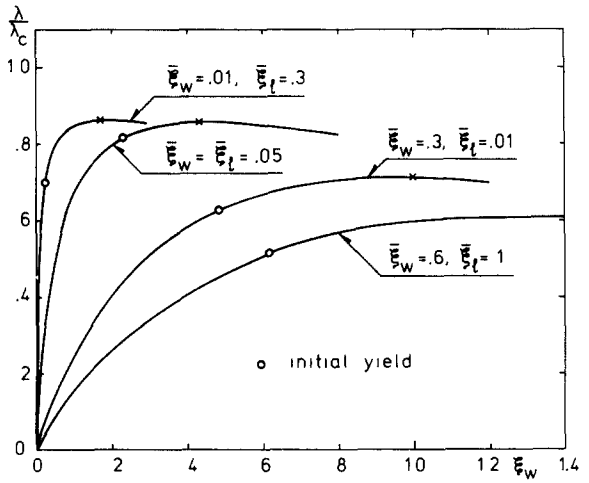

Fig. 11. Load vs wide column mode displacement for continuous panel on multiple supports with simultaneous elastic bifurcation in wide column and local buckling modes ($\sigma_y/E = 0{\cdot}00195$, $\sigma_c/\sigma_y = 0{\cdot}909$, $n = 10, \alpha = 0{\cdot}7165, a/b = 4, e/b = 0{\cdot}1, (A_s + hb)/b^2 = 0{\cdot}0256, \nu = 0{\cdot}3$).

mitigated by the fact that half of the bays are forced in the direction in which no mode interaction occurs. On the other hand an elastic–plastic panel on two supports is so sensitive to column mode imperfections of both signs, that no mitigating effect is found for the elastic–plastic continuous panel on multiple supports.

In Figs. 9–11 the behaviour is given of continuous panels corresponding to the panels in Figs. 5, 6 and 8, respectively. The computations have only been carried out for positive imperfections since the continuous panel behaves symmetrically with respect to both ξ_w and ξ_l. The numerically computed plastic post-bifurcation behaviour shown in Figs. 9 and 10 and the asymptotic results given in Section 4 agree in predicting that the maximum load is only slightly above the bifurcation load, although the maximum loads and the corresponding mode deflection amplitudes (4.8) obtained from the truncated series (4.1) are generally a little smaller and a great deal smaller, respectively, than the numerical results. Also there is good agreement between the asymptotically predicted shapes of the elastic unloading zones and the numerically computed unloading zones.

A considerable imperfection-sensitivity is found both for the continuous panels in Figs. 9 and 10 that bifurcate in the plastic range and for the continuous panel in Fig. 11 that bifurcates in the elastic range. In Fig. 9 the panel with imperfections $\bar{\xi}_w = 0{\cdot}6$, $\bar{\xi}_l = 0{\cdot}1$ has a maximum load about the average of the maxima corresponding to $\bar{\xi}_w = \pm 0{\cdot}6$, $\bar{\xi}_l = 0{\cdot}1$ in Fig. 5, and doubling the imperfection amplitudes further diminishes the carrying capacity significantly. As was the case in Fig. 6, the smaller strain hardening parameter $n = 4$ in Fig. 10 increases the bifurcation stress and the mode amplitudes at which maxima occur, but hardly changes the imperfection-sensitivity. The panel in Fig. 11 is considerably more imperfection-sensitive than the panels in Figs. 9 and 10. A part of the reason for this is that the loads get closer to the elastic bifurcation load so that the mode displacements prior to initial yielding are relatively large.

In panels simply supported on the two edges and with $\bar{\xi}_w = 0$ a local mode imperfection gives a rapid growth of ξ_w. The same does not happen for the continuous panels on several transverse supports as shown by the curves $\bar{\xi}_w = 0{\cdot}01$, $\bar{\xi}_l = 0{\cdot}3$ in Figs. 9 and 11. In fact for the continuous panels in these two figures a case with $\bar{\xi}_w = 0$, $\bar{\xi}_l \neq 0$ will have no column mode displacements

before they are introduced at a bifurcation point somewhat below the bifurcation point for the perfect structure.

In general these numerical examples show that the imperfection-sensitivity of integrally stiffened elastic–plastic panels is considerable, both when they bifurcate in the plastic range and when the yield stress is a little above the elastic bifurcation stress. For the panel over only one bay the imperfection-sensitivity due to mode interaction is increased by plasticity, and furthermore plasticity gives a severe sensitivity to negative column mode imperfections. These two different causes of imperfection-sensitivity are both present in the continuous multiply supported panel with the result that this structure is also rather imperfection-sensitive.

REFERENCES

1. A. van der Neut, The interaction of local buckling and column failure of thin-walled compression members. *Proc. 12th Int. Congr. Appl. Mech., Stanford University* 1968. Springer-Verlag, Berlin (1969).
2. W. T. Koiter and G. D. C. Kuiken, The interaction between local buckling and overall buckling on the behaviour of built-up columns. *Delft Lab. Rep.*—WTHD 23 (May 1971).
3. J. M. T. Thompson and G. M. Lewis, On the optimum design of thin-walled compression members. *J. Mech. Phys. Solids* **20**, 101 (1972).
4. V. Tvergaard, Imperfection-sensitivity of a wide integrally stiffened panel under compression. *Int. J. Solids Structures* **9**, 177 (1973).
5. V. Tvergaard, Influence of post-buckling behaviour on optimum design of stiffened panels. *Int. J. Solids Structures* **9**, 1519 (1973).
6. W. T. Koiter and M. Pignataro, An alternative approach to the interaction between local and overall buckling in stiffened panels. (to appear in *Proc. IUTAM Symposium on Buckling of Structures*, Harvard University, June 17–21, 1974).
7. A. van der Neut, Mode interaction with stiffened panels, (to appear in *Proc. IUTAM Symp. on Buckling of Structures*, Harvard University, 17–21 June 1974).
8. J. M. T. Thompson, J. D. Tulk and A. C. Walker, An experimental study of imperfection-sensitivity in the interactive buckling of stiffened plates, (to appear in *Proc. IUTAM Symp. on Buckling of Structures*, Harvard University, 17-21 June 1974).
9. T. R. Graves Smith, The effect of initial imperfections on the strength of thin-walled box columns. *Int. J. Mech. Sci.* **13**, 911 (1971).
10. V. Tvergaard and A. Needleman, Mode interaction in an eccentrically stiffened elastic–plastic panel under compression. (to appear in *Proc. IUTAM Symp. on Buckling of Structures*, Harvard University, 17–21 June 1974).
11. J. W. Hutchinson, Post-bifurcation behavior in the plastic range. *J. Mech. Phys. Solids* **21**, 163 (1973).
12. J. W. Hutchinson, Plastic buckling. *Adv. Appl. Mech.* **14**, to be published.
13. R. Hill, A general theory of uniqueness and stability in elastic–plastic solids. *J. Mech. Phys. Solids* **6**, 236 (1958).
14. R. Hill, Bifurcation and uniqueness in non-linear mechanics of continua. *Problems of Continuum Mechanics*, pp. 155–164. S.I.A.M. Philadelphia (1961).
15. W. T. Koiter, Over de stabiliteit van het elastisch evenwicht. Thesis, Delft, H. J. Paris, Amsterdam (1945). English translation issued as NASA TT F-10, 833 (1967).
16. T. Kawai and H. Ohtsubo, A method of solution of geometrically nonlinear problems of elastic plates. (in Japanese). *J. Soc. of Naval Architects of Japan* (126), 235 (1969).
17. T. Kawai, Finite element analysis of the geometrically nonlinear problems. *Recent Advances in Matrix Methods of Structural Analysis and Design*, pp. 383–414. University of Alabama Press (1971).
18. H. Ohtsubo, A method of elastic–plastic analysis of largely deformed plate problems. *Advances in Computational Methods in Structural Mechanics and Design* (Edited by J. T. Oden *et al.*), pp. 439–456. University of Alabama Press (1972).
19. O. C. Zienkiewicz, *The Finite Element Method in Engineering Science.* 2nd Edn. McGraw-Hill, London (1971).
20. A. Needleman, Post-bifurcation behaviour and imperfection-sensitivity of elastic–plastic circular plates. *Int. J. Mech. Sci.* to be published.
21. J. W. Hutchinson, Imperfection-sensitivity in the plastic range. *J. Mech. Phys. Solids* **21**, 191 (1973).